Glycoconjugate Journal 16, 437–456 (1999)

Characterisation of tissue-specific oligosaccharides from rat brain and kidney membrane preparations enriched in Na^+,K^+-ATPase

Richard A.C. Clark[1], Bernhard Küster[1,2], Mounja Benallal[3], Beatrice M. Anner[3], Raymond A. Dwek[1], David J. Harvey[1] and David R. Wing[1]*

[1]*Glycobiology Institute, Department of Biochemistry, University of Oxford, South Parks Road, Oxford OX1 3QU, UK*
[2]*Center for Experimental BioInformatics, Odense University, Odense, Denmark*
[3]*Department of Pharmacology, Geneva University Medical School, CH-1211 Geneva 4, Switzerland*

The organ-specific nature of the glycosylation of Na^+,K^+-ATPase-enriched preparations from kidney and brain tissues has earlier been indicated by the use of lectin-staining techniques. Na^+,K^+-ATPase is ubiquitous and abundant, and subject to upregulation during cell-division and in certain pathological conditions. Lectins specific for the different carbohydrates displayed by the Na^+,K^+-ATPases may, therefore, be useful carriers/mediators in tissue-specific targeting. N-linked oligosaccharides purified from Na^+,K^+-ATPase-enriched preparations from rat brain and kidney were consequently characterised in detail in this study using weak anion exchange and normal phase HPLC (combined with serial glycosidase digestions) and matrix-assisted laser desorption/ionisation mass spectrometry. The oligomannose series of glycans were most abundant in the brain tissue preparation and this contrasted with the renal-associated oligosaccharides that were dominated by families of tetra-antennary glycans (with/without a core fucose) with up to four lactosaminylglycan residues in either branched or linear formation.

Keywords: **glycosylation/Na^+,K^+-ATPase/oligomannose/polylactosamine/tissue-specific**

Abbreviations: **2-AB, 2-aminobenzamide; AMOG, adhesion molecule on glia; ATP, adenosine triphosphate; BSA, bovine serum albumin; CAM, calcium/calmodulin-dependent protein kinase; CNS, central nervous system; DSA, *Datura stramonium* agglutinin (lactosamine and sialic acid recognition); EDTA, ethylenediaminetetra-acetic acid; Gal, galactose; GlcNAc, N-acetyl-D-glucosamine; GNA, *Galanthus nivalis* agglutinin (oligomannosidic recognition); GnT, *N*-acetylglucosaminyltransferase; GU, glucose unit; HPLC, high performance liquid chromatography; MALDI, matrix-assisted laser desorption/ionisation; $(Man)_{5-9}$, oligomannose-type glycan series with 5–9 mannose residues; Man_1, Manβ1-4GlcNAcβ1-4 GlcNAc; Man_3, trimannose-chitobiose core; Man_3F, trimannose-chitobiose core with fucose on reducing terminal GlcNAc; MS, mass spectrometry; NP, normal phase; PBS, phosphate buffered saline; PNGase F, protein-N-glycosidase F; PVDF, poly(vinylidene difluoride); SDS-PAGE, sodium dodecyl sulphate polyacrylamine gel electrophoresis; TOF, time-of-flight; Tris, 2-amino-2-hydroxymethylpropane-1,3 diol; WAX, weak anion exchange**

Introduction

The Na^+,K^+-ATPase is a ubiquitous membrane-bound enzyme which is responsible for the maintenance of Na^+ and K^+ concentration gradients using ATP in a coupled active transport process [1]. These chemical gradients can be used for the transport of other solutes such as glucose, amino acids and other nutrients into cells. Ionic gradients regulated by Na^+,K^+-ATPases in the kidneys and intestines are used to control electrolyte movement and fluid re-absorption. Na^+,K^+-ATPase also helps to control cell volume as it controls solute concentrations, thus having an effect on osmotic forces, leading to cell shrinkage or swelling.

Na^+,K^+-ATPases are composed of two non-covalently linked subunits (α and β in an equimolar ratio, the minimal functional unit being an αβ dimer. Only α subunits that assemble with β subunits in the endoplasmic reticulum are fully functional, stably expressed and transported to the plasma membrane [2,3]. The α subunit is the larger of the two at approximately 113 kDa and is thought to be a complex membrane protein of the class IV type with several

*To whom correspondence should be addressed. Tel. No. (44)-(0)1865-275756; Fax No. (44)-(0)1865-275216

membrane spanning domains [4]. The smaller β subunit (~55 kDa) is thought to be a type II integral membrane protein with a short N terminal cytoplasmic tail, one transmembrane domain and a large extracellular C terminal segment [1,5]. The α subunit contains all the functional domains of the enzyme, namely binding sites for ATP, phosphate, cations and specific cardiac glycoside inhibitors suggesting that this subunit has the major catalytic role. The role of the β subunit is less well defined but evidence suggests a function in the maturation of the enzyme and intracellular transport to the plasma membrane [2]. Assembly of the β subunit is required for α to assume the correct conformation necessary for its function and exit from the endoplasmic reticulum. The β subunit may also function indirectly in the modulation of Na^+,K^+-ATPase activity. This is supported by Gloor et al. [6] who identified the β-2 subunit as the adhesion molecule on glia (AMOG). The α subunit is known to exist in at least 3 isoforms (α-1, α-2, α-3) coded by one family of genes whereas the β subunit family encodes β-1 and β-2 isoforms. Na^+,K^+-ATPase subunit isoforms are tissue-specific [7], for example, rat brain contains α-1, α-2, α-3, β-1 and β-2 whilst rat kidney contains α-1 and β-1 [8].

The glycosylation of Na^+,K^+-ATPase has been shown to be organ-specific as illustrated by the use of lectins in the work of Benallal and Anner [8]. Since the enzyme is known to be strongly up-regulated during cell division and in certain pathological situations, such as virus infection, carbohydrate-specific lectins that recognize the glycoconjugates of this abundant protein carry the potential for tissue-specific targeting, advantageous in therapeutics. Thus a knowledge of the specific carbohydrate structures underlying the differential lectin recognition between tissues is essential for an assessment of the potential for targeting the glycans of this abundant protein. In the present study, kidney and brain membrane preparations enriched in Na^+,K^+-ATPase, are analysed in non-pathological conditions in the rat.

An investigation of the major oligosaccharides at each of the three N-glycosylation sites in the β subunit has been performed by Treuheit et al. [9] for Na^+,K^+-ATPase from lamb and dog kidney. Few differences in glycosylation were observed between the sites, most glycans being tetra-antennary structures with/without repeating *N*-acetyl-lactosaminoglycan units. Oligosaccharide analysis was limited to characterisation through compositional data from mass spectrometry. Thus it was not possible to distinguish between structures having the same monosaccharide composition, particularly with respect to the form of the *N*-acetyl-lactosamine unit extensions. In this study structural information was obtained from extensive serial glycosidase digestions with monitoring by HPLC combined with on-line fluorescence detection. This gave high sensitivity and quantitation, and was combined with data obtained from matrix-assisted laser desorption/ionisation mass spectrometry (MALDI-MS). As a result, a more rigorous approach to the structural identification of the carbohydrate moieties in both brain and kidney Na^+,K^+-ATPase-enriched preparations is reported than has hitherto been described, so that a direct comparison between the two tissues could be made.

Materials and methods

Materials

All reagents were of the highest purity commercially available. All enzymes, including *Bacteroides fragilis* endo β-galactosidase, were purchased from Oxford GlycoSciences (Abingdon, UK) except *Charonia lampas* α-fucosidase which was obtained from Dr. T. Butters, Glycobiology Institute, Oxford. The rabbit anti-sera to the α-1, α-2, α-3, β-1, β-2 isoform sub-units of rat Na^+,K^+-ATPase were from Upstate Biotechnology Inc. (New York, USA). The materials used for mass spectrometry in-gel digestion studies were exactly as outlined in Küster et al. [10].

Preparation of Na^+,K^+-ATPase

Na^+,K^+-ATPase-enriched fractions, prepared as described by Dzhandzhugazyan and Jorgensen [11], were suspended in 1% sucrose, 25 mM imidazole, 1 mM Tris-EDTA, pH 7.5. Protein was estimated using a bicinchoninic acid assay (Pierce, Rockford, IL, USA) and samples were kept at −70 °C until required.

Analytical SDS PAGE and electrophoretic transfer of proteins

Analytical SDS PAGE (BioRad Mini-PROTEAN II system) was performed at 200V using either 8 or 6% (w/v) acrylamide separating gels for Western blotting and N-terminal sequencing respectively [12]. Electrophoresis was also performed using a 15 × 15cm size vertical gel (0.75 mm thick) under the same conditions as the mini-gel but running at a constant 25 or 30 mA. Electroblotting of glycoproteins for Western blotting was performed onto nitrocellulose (Schleicher and Schuell, Dassel, Germany) using a BioRad Transblot SD semi-dry transfer cell at 25 V for 1 hour (transfer buffer 25 mM Tris, 192 mM glycine, 20% (v/v) methanol, pH 8.2). Electroblotting of glycoproteins for N-terminal sequencing was performed onto PVDF membranes (Immobilon-P; Millipore Co. Bedford, MA, USA) as above but reducing the transfer time to 45 min.

Western blotting

The electroblotted membranes were blocked overnight at 4 °C in 5% (w/v) non-fat milk powder in PBS containing 0.05% (v/v) Tween-20 (milk/PBST) and a 1:50 dilution of normal swine serum (Vector Labs., Peterborough, UK). After washing in milk/PBST the immunoblots were incubated for 3 hours at room temperature with a 1:1000 dilu-

tion of primary antibodies to either the α-1, α-2, α-3, β-1 or β-2 isoform subunits of rat Na^+,K^+-ATPase in blocking solution (see above). After being washed in milk/PBST the membranes were incubated for 1 hour at room temperature with swine anti-rabbit IgG secondary antibodies (Dako A/S, Glostrup, Denmark) conjugated to horseradish peroxidase (dilution of 1:1000 in milk/PBST). The membranes were washed in PBST, incubated in chemiluminescent detection solution (Pierce, Rockford, Il, USA) and exposed to photographic film.

Protein characterisation

a) N-Terminal Sequencing. PVDF blots from the brain and kidney Na^+,K^+-ATPase-enriched preparations (see above) were used for N-terminal sequencing essentially as described by Matsudaira [13]. The excised bands were placed in the sequencer (Beckman LF 3000 Protein Sequencer, Beckman Instruments Inc., Fullerton, California, USA) for N-terminal sequencing by Edman Degradation using pre-column phenylisothiocyanate derivatisation.

b) Identification by MS. Peptide mass maps were derived from individual protein-band regions of the SDS gels by in-gel trypsin digestion (post-PNGase F) and subsequent MALDI-MS analysis using a modified Bruker Reflex time-of-flight (TOF) mass spectrometer [14].

In addition, peptides were sequenced by nano-electrospray tandem MS on a PE Sciex 300 triple quadrupole mass spectrometer as described earlier [15]. The peptide mass and partial sequence information that was obtained was searched against a non-redundant sequence database maintained and updated regularly at the European Bioinformatics Institute (EBI), Hinxton Hall, Cambridge, UK.

Oligosaccharide release and preparation for analysis

a) From total Na^+,K^+-ATPase-enriched preparations. Approximately 500 μg of brain protein and 600 μg of renal protein were acetone-precipitated at −20 °C and the pelleted material was washed twice in pre-cooled (−20 °C) acetone/glacial acetic acid/triethylamine/water (17:1:1:1, v/v/v/v). Samples were suspended in water, frozen and lyophilised overnight. Oligosaccharides were released by anhydrous hydrazinolysis and purified as described by Ashford et al. [16]. Hydrazinolysis conditions were optimal for the liberation of N-linked glycans [17]. The purified oligosaccharides were fluorescently labelled with 2-aminobenzamide (2-AB) by the procedure of Bigge et al. [18] using a Signal Labelling kit from Oxford GlycoSciences (Abingdon, UK). Samples were kept at −20 °C in 1 ml of water until used for analysis by HPLC.

b) From gel-separated protein bands. 30 μg each of the brain and kidney Na^+,K^+-ATPase-enriched preparations were subjected to SDS-PAGE (BioRad system, see above, at 200V) using the method of Laemmli [12] and a 12.5% (w/v) acrylamide resolving gel containing 0.1% (w/v) bis(N,N′-methylene-bis-acrylamide). After visualisation with Coomassie blue and partial destaining, the high and low molecular weight bands (associated with the α and β subunits of Na^+,K^+-ATPase) were excised. N-glycans were released from the reduced and alkylated (glyco) protein bands, in gel, by PNGase F (100 U/ml) as described by Küster et al. [10] and were desialylated with *Arthrobacter ureafaciens* neuraminidase (1 U/ml). After incubation overnight at 37 °C, the released glycans were extracted and cleaned prior to mass spectrometry as described by Küster et al. [10]. In this case no labelling of the glycans was required.

High-performance liquid chromatography

Weak anion exchange (WAX) HPLC of the fluorescently labelled oligosaccharides was performed essentially as described by Guile et al. [19]. Normal phase HPLC was modified from Guile et al. [20] using a gradient of 50 mM ammonium formate, pH 4.4 and a 4.6 × 250 mm GlycoSep-N HPLC column (Oxford GlycoSciences). Solvent A was 50 mM ammonium formate, pH 4.4, solvent B was acetonitrile. An initial linear gradient of 35% (v/v) A to 58% (v/v) A over 92 min was followed by 58–100% (v/v) A over the next 3 min at a flow rate of 0.4 ml/min. The flow rate was then increased to 1 ml/min over the next 2 min and the column was washed in 100% (v/v) A for 5 min before being re-equilibrated in 35% (v/v) A for 20 min.

Glycosidase digestions

Glycosidase digestions were performed on 2-AB labelled acidic sugars from WAX HPLC, neutral glycans from normal phase HPLC and on 2-AB labelled standards. Microscale digests were performed using 15 μl enzyme as indicated: *Arthrobacter ureafaciens* sialidase (4 U/ml), jack bean α-mannosidase (40 U/ml), almond meal α-fucosidase (3 mU/ml), *Bacteriodes fragilis* endo β-galactosidase (1 mU/ml), bovine testes β-galactosidase (2 U/ml), jack bean β-N-acetylhexosaminidase (10 U/ml), and *Charonia lampas* α-fucosidase (0.8 U/ml). Digests were performed in the following buffer: 50 mM citrate/phosphate, 0.15 M NaCl, 0.25 mg/ml BSA pH 4.5 except jack bean α-mannosidase (as above plus 0.2 mM zinc acetate) and *A. ureafaciens* sialidase (20 mM ammonium acetate pH 5.0). Incubations, in an atmosphere of toluene, were for 18–24 hours at 37 °C. Proteins were removed after every digest by spotting samples onto Pro-Spin 0.45 μm nitrocellulose microcentrifugal filters (Radleys, Saffron Walden, UK). Glycans were eluted in 5% (v/v) aqueous acetonitrile. Samples were dried *in vacuo,* then dissolved in either 80% acetonitrile/water (v/v) before injection onto normal phase HPLC or water prior to injection onto WAX HPLC.

Mass spectrometry of N-glycans from SDS-PAGE separated protein bands

MALDI-mass spectra were acquired on a Perseptive Biosystems Voyager Elite reflectron mass spectrometer using 2,5-dihydroxybenzoic acid as the matrix. Reported masses correspond to the monoisotopic masses of the respective sodiated molecules.

Results

HPLC and glycosidase digests

Oligosaccharides released by hydrazinolysis from the Na^+,K^+-ATPase-enriched preparations from brain and kidney were fluorescently labelled with 2-AB and subjected to weak anion exchange (WAX) HPLC (Figure 1). A higher proportion of neutral glycans, eluting at the void volume (V), was apparent for the brain than for the kidney sample (54 and 33% respectively). Both contained species which co-eluted with mono-, di-, tri-, and tetrasialylated standards (Figure 1).

A portion of the natural neutral glycans was subjected to normal phase (NP) HPLC in each case (profiles not shown, but form a significant contribution to the profiles of 'natural neutral' and 'neutralised' glycans in (a) of both Figures 2 and 3). The main components for the brain sample were the oligomannosidic glycans $(Man)_{5-9}$, which together constituted 36% of the total (neutral + acidic) oligosaccha-

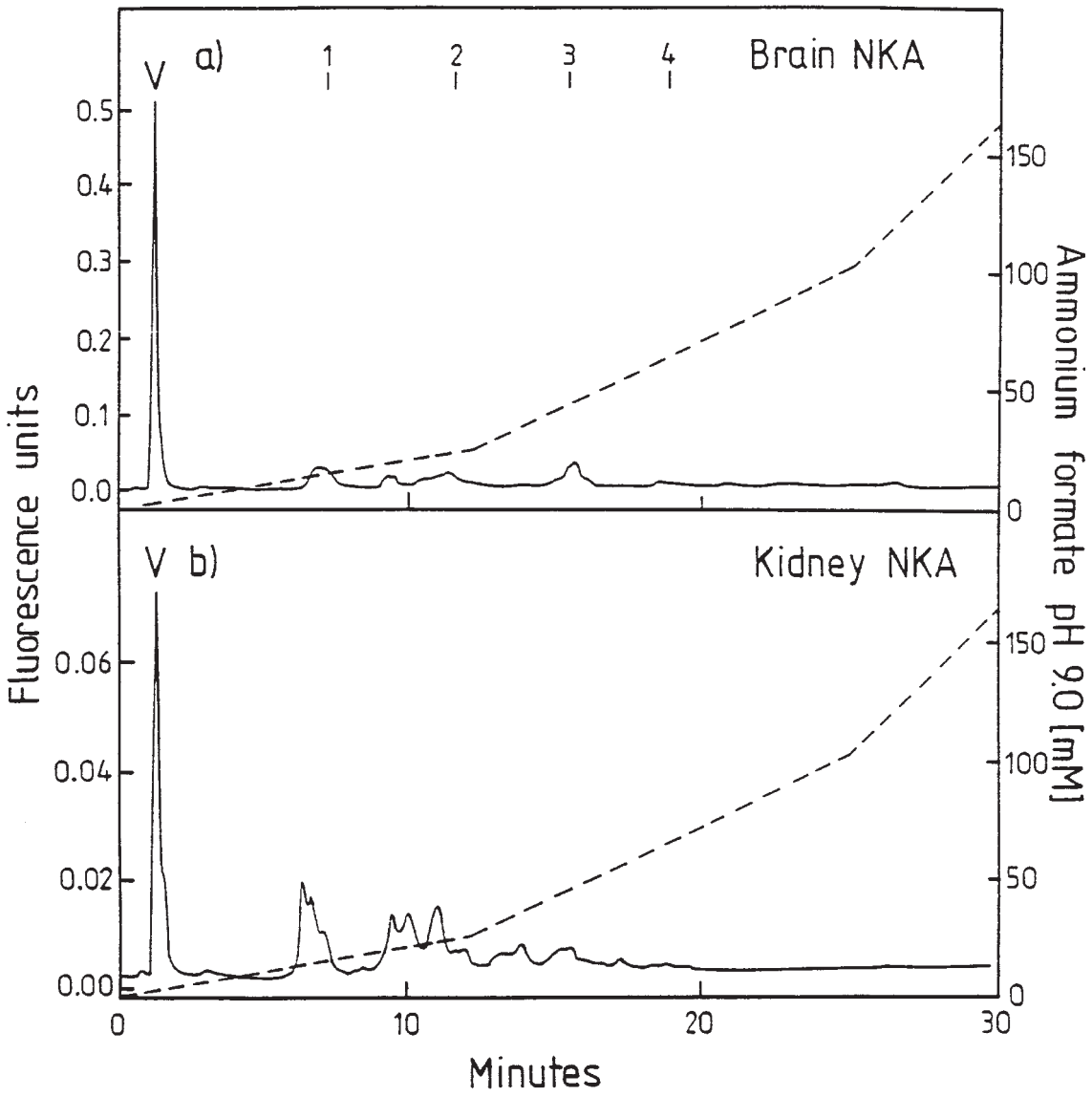

Figure 1. Weak anion exchange HPLC of total released glycans from (a) brain Na^+,K^+-ATPase and (b) kidney Na^+,K^+-ATPase-enriched preparations. Elution positions marked 1, 2, 3, 4 indicate retention times for mono-, di-, tri-, tetra-sialylated N-linked glycans from fetuin. V: elution peak of neutral glycans immediately after column void.— — —: ammonium formate concentration. NKA = Na^+,K^+-ATPase.

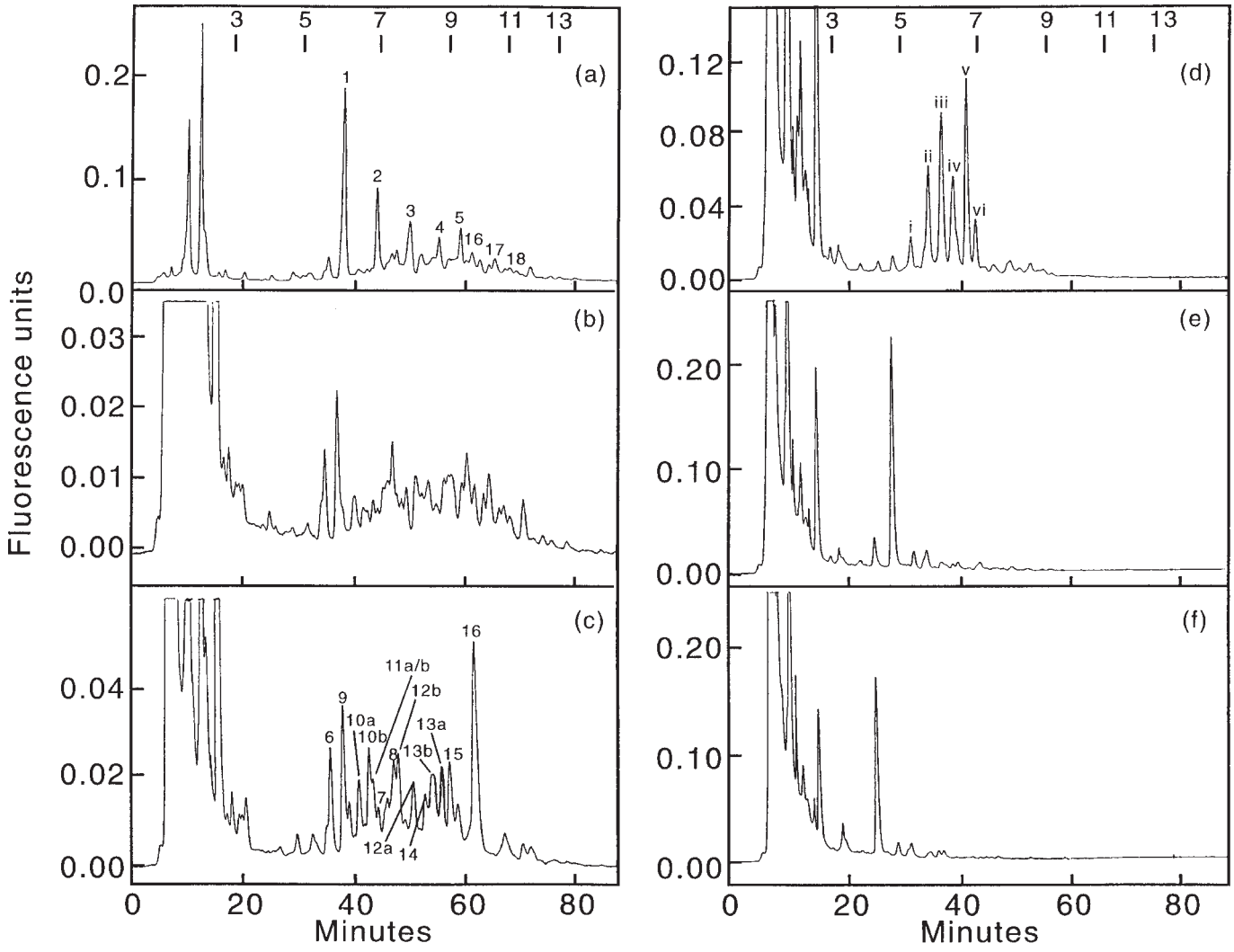

Figure 2. The sequential glycosidase digestion of oligosaccharides from the brain Na^+,K^+-ATPase preparation analysed by normal phase HPLC. (a) the neutralised fraction (natural neutral plus desialylated acidic glycans) plus (b) jack bean α-mannosidase, plus (c) almond meal α1-3/α1-4 fucosidase, plus (d) bovine testes β-galactosidase, plus (e) jack bean β-*N*-acetylhexosaminidase, plus (f) *Charonia lampas* α-fucosidase. Numbered notations at the top of the figure indicate elution positions of glucose oligomers (normal phase glucose units, NPGU). Peaks with Arabic numerals (1–18) indicate the elution positions of compounds nos. 1–18, respectively, given in Table 2. Peaks with Roman numerals (i–vi) indicate the elution positions of intermediate digestion products described in Figure 4 and in the text.

rides. This contrasted with a value of only 17% for the kidney. Individual identities for $(Man)_{5-9}$ were confirmed by digestion with jack bean α-mannosidase and sequential NP-HPLC and were supported by the isobaric monosaccharide composition data, obtained by MALDI-MS, shown below (Table 1). Man_5 and Man_6 were most abundant, their percentage composition relative to other natural neutral N-glycans being 29% and 13% respectively for the brain preparation and 12 & 16% respectively for the kidney. Progressive declines in relative abundance were observed from Man_7 to Man_9 in both the brain and kidney samples (to as low as 5–6% in each tissue for Man_9).

Another portion of the 2-AB-labelled oligosaccharides obtained from both the brain and kidney samples was desialylated using *Arthrobacter ureafaciens* sialidase and then subjected to WAX HPLC. All the retarded, anionic peaks observed in Figure 1 were neutralised by this treatment, so that only a peak at the column void was observed for each tissue (data not shown). These neutralised glycans, together with those 'natural neutral' oligosaccharides already present in the void peak, were analysed by NP HPLC (Figures 2a and 3a for the brain and kidney samples, respectively). Sequential glycosidase digestions were performed as shown in Figures 2b–f and 3b–f for the two tissue samples. The numbered peaks represent glycans present, and identified, in the original neutral/desialylated sample and can be cross-referenced to the compound numbers listed below in Table 2 (brain) and Table 3 (kidney).

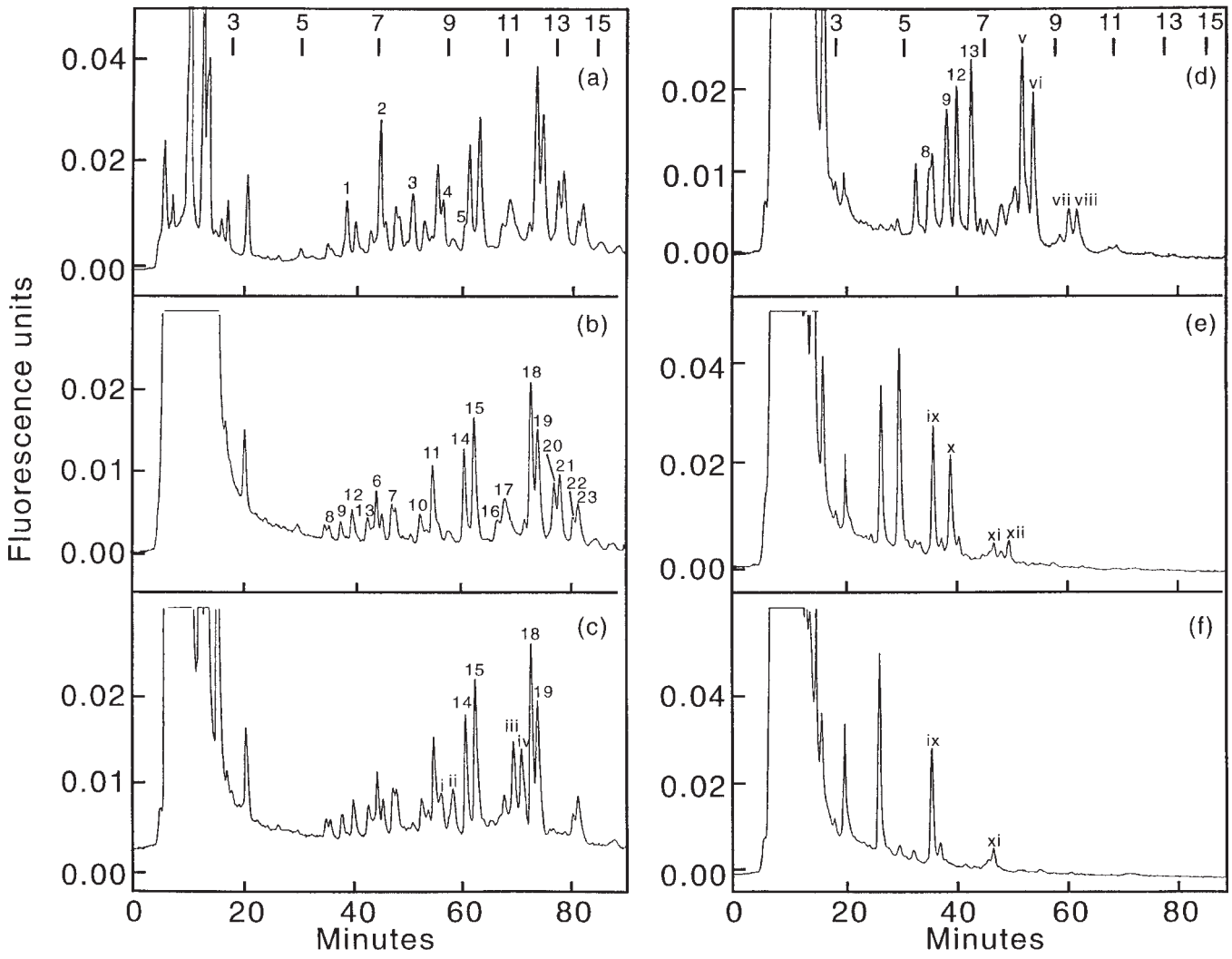

Figure 3. The sequential glycosidase digestion of oligosaccharides from the kidney Na^+,K^+-ATPase preparation analysed by normal phase HPLC. (a) the neutralised fraction (natural neutral plus desialylated acidic glycans) plus (b) jack bean α-mannosidase, plus (c) endo β-galactosidase, plus (d) bovine testes β-galactosidase, plus (e) jack bean β-*N*-acetylhexosaminidase, plus (f) *Charonia lampas* α-fucosidase. Numbered notations at the top of the figure indicate elution positions of glucose oligomers (normal phase glucose units, NPGU). Peaks with Arabic numerals (1–23) indicate the elution positions of compound nos. 1–23, respectively, given in Table 3. Peaks with Roman numerals (i–xii) indicate the elution positions of intermediate digestion products described in Figure 5. Peak numbering is used independently between the kidney- and brain-derived samples.

(i) Glycosidase digestions of the brain Na^+,K^+-ATPase preparation. The major carbohydrate structures in the NP HPLC chromatogram of natural neutral and neutralised N-glycans (Figure 2a) were analysed through changes in NPGU values following sequential glycosidase digestions, together with reference to the isobaric monosaccharide compositions of glycans detected by MALDI-MS (Table 1). The major peaks, assigned as $(Man)_{5-9}$ (labelled 1–5 in Figure 2a), were completely digested by jack bean α-mannosidase to give a peak at 2.41 NPGU (off scale and adjacent to the void material, Figure 2b) consistent with the generation of Man_1. Additional results, below, from MALDI-MS (Table 1) further supported the presence of the oligomannosidic glycans, $(Man)_{5-9}$, as reported above.

Digestion of the remaining major (complex type) glycans (Figure 2c–f) is summarised in Figure 4 with interpretation depending, not only on the NPGU values of the main core oligosaccharide structures, but also on the significant earlier changes in NPGU values obtained with specific glycosidase digestions of the outer monosaccharide residues, as published in Guile et al. [20]. Thus, after almond α1-3/4 fucosidase digestion, the profile is dominated by the relative increase in abundance of the assigned core-fucosylated tetra-antennary N-glycan (peak 16, Fig. 2c) arising from digestion of the outer-arm fucosylated (Lewis x-containing) members of that family (peaks 17 and 18 in Figure 2a). Their structural assignments are shown in Table 2.

Digestion with bovine testes β-galactosidase produced

Table 1. Isobaric monosaccharide compositions of N-glycans from SDS-PAGE separated high and low molecular weight protein bands of brain and kidney Na^+,K^+-ATPase-enriched preparations.

Mass[1]					
Observed					
Brain		*Kidney*			
High MW	*Low MW*	*High MW*	*Low MW*	*Calc.*	*Comp.*[2]
1257.4	1257.4	1257.5	—[3]	1257.4	H_5N_2
1419.5	1419.5	1419.5	—	1419.5	H_6N_2
1485.5	1485.4	—	—	1485.5	$H_3N_4F_1$
1542.6	1542.2	1542.5	—	1542.6	H_3N_5
1581.5	1581.5	1581.5	1581.6	1581.5	H_7N_2
1647.5	1647.5	—	—	1647.6	$H_4N_4F_1$
1663.5	1663.5	1663.5	1663.6	1663.6	H_5N_4
1688.6	1688.5	—	—	1688.6	$H_3N_5F_1$
1704.5	1704.6	1704.5	—	1704.6	H_4N_5
1743.5	1743.5	1743.5	—	1743.6	H_8N_2
1752.5	1752.6	—	—	1752.6	$H_5N_3F_2$
1768.5	1768.4	—	—	1768.6	$H_6N_3F_1$
1793.6	1793.4	—	—	1793.6	$H_4N_4F_2$
1809.6	1809.6	—	—	1809.6	$H_5N_4F_1$
1825.6	1825.6	1825.5	—	1825.6	H_6N_4
1850.6	1850.6	1850.2	—	1850.6	$H_4N_5F_1$
—	1866.7	1866.6	—	1866.7	H_5N_5
1905.6	1905.5	1905.5	—	1905.6	H_9N_2
1955.7	1955.5	—	—	1955.7	$H_5N_4F_2$
1996.7	1996.6	—	—	1996.7	$H_4N_5F_2$
2012.7	2012.6	2012.6	—	2012.7	$H_5N_5F_1$
2028.8	2028.7	2028.7	2028.7	2028.7	H_6N_5
—	2053.7	—	—	2053.7	$H_4N_6F_1$
—	2069.6	2069.7	—	2069.7	H_5N_6
2158.9	2158.7	—	—	2158.8	$H_5N_5F_2$
2174.9	2174.7	—	2174.7	2174.8	$H_6N_5F_1$
—	2199.7	—	—	2199.8	$H_4N_6F_2$
2216.0	2215.7	—	—	2215.8	$H_5N_6F_1$
2232.0	2231.8	—	—	2231.8	H_6N_6
2305.0	2304.8	—	—	2304.8	$H_5N_5F_3$
2321.1	2320.7	—	—	2320.8	$H_6N_5F_2$
—	2361.7	—	—	2361.9	$H_5N_6F_2$
2377.9	2377.7	—	—	2377.9	$H_6N_6F_1$
2394.0	2393.8	—	2393.8	2393.8	H_7N_6
2507.7	2507.5	—	—	2507.9	$H_5N_6F_3$
2534.0	2523.8	—	—	2523.9	$H_6N_6F_2$
2540.0	2539.8	—	2539.7	2539.9	$H_7N_6F_1$
2613.4	2613.3	—	—	2613.0	$H_6N_5F_4$
2670.3	2670.1	—	—	2670.0	$H_6N_6F_3$
2686.0	2685.7	—	—	2686.0	$H_7N_6F_2$
—	—	—	2758.9	2759.0	H_8N_7
—	2831.6	—	—	2832.0	$H_7N_6F_3$
—	—	—	2905.0	2905.0	$H_8N_7F_1$
—	—	—	3123.9	3124.1	H_9N_8
—	—	—	3270.0	3270.2	$H_9N_8F_1$
—	—	—	3489.4	3489.2	$H_{10}N_9$

[1]Monoisotopic mass of the MNa^+ ion.
[2]H = hexose (galactose, mannose), N = HexNAc (GlcNAc), F = deoxyhexose (fucose).
[3]— = Not detected.

Table 2. Assignment of glycan structures from total Na^+,K^+-ATPase-enriched preparation of brain.

Isobaric composition	*NP HPLC glucose units*[a]	*Structure*[b]	*Ref.#*[c]
H5 N2	6.15 (6.16)	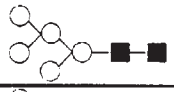	1
H6 N2	7.04 (7.05)	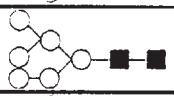	2
H7 N2	7.94 (7.91)	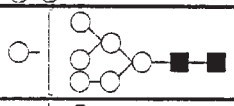	3
H8 N2	8.80 (8.81)	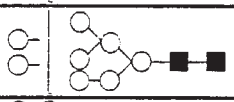	4
H9 N2	9.48 (9.49)	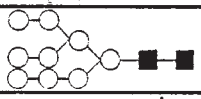	5
H3 N4 F	5.76 (5.70)	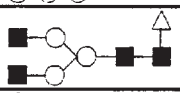	6
H5 N4	7.03 (7.00)	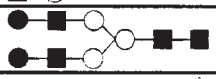	7
H5 N4 F	7.46 (7.43)		8
H3 N5 F	6.09 (6.04)		9
H4 N5	6.51 (6.51)	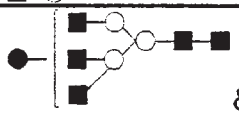	10a
	6.79 (6.76)		10b
H4 N5 F	6.90 (6.90)	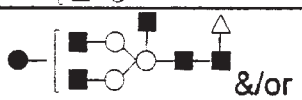	11a
	6.90 (6.91)	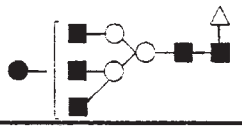	11b
H5 N5 F	8.02 (8.06)	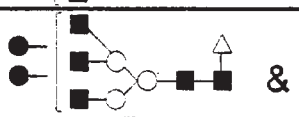	12a
	7.59 (7.53)		12b
H6 N5 F	8.85 (8.88)	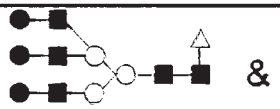	13a
	8.59 (8.61)	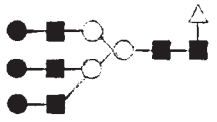	13b

Table 2. *(continued)*

Isobaric composition	*NP HPLC glucose units*[a]	*Structure*[b]	*Ref.#*[c]
H5 N6 F	8.35 (8.35)	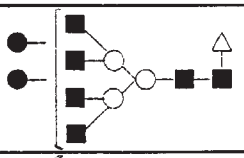	14
H6 N6 F	9.10 (9.08)	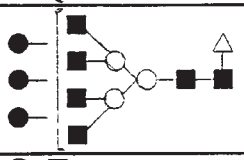	15
H7 N6 F	9.89 (9.93)	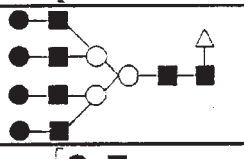	16
H7 N6 F2	10.65 (10.71)	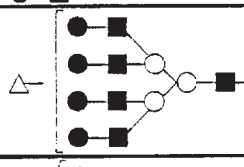	17
H7 N6 F3	11.46 (11.51)	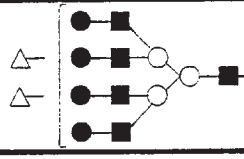	18

[a]The NP HPLC glucose units of standards were listed in parenthesis where these data were available. If these data were not available the glucose units have been predicted using the data in Guile et al., 1996.
[b]The squares represent N-acetyl glucosamine, white circles mannose, black circles galactose and triangles fucose.
[c]The reference number cross-references this table with the oligosaccharide peaks of Figure 2.

six main peaks, not entirely resolved by NP HPLC, containing the following de-galactosylated N-glycan structures: bi- and tri- antennaries +/− core fucose, tetra-antennary with core fucose and the bi-antennary with both core fucose and a bisecting GlcNAc (Figure 2d, i–vi; and Figure 4). Structural assignments of (mainly) parent compounds are given in Table 2. (Assignment of the monogalactosylated (2,6)tri-antennary glycan without core fucose (structure 10b, Table 2) is tentative as its digestion product eluted with other products contained in (iii) (Figures 2d and 4)).

Other 'core' glycans found after degalactosylation were also not entirely resolved : thus peak (ii) (Figure 2d) contained the degalactosylated (2,4)tri-antennary structure (from 10a in Table 2) as a shoulder (at 5.66 NPGU) on the degalactosylated bi-antennary structure containing a core fucose (at 5.70 NPGU, and obtained from structure 8 in Table 2). Also, the degalactosylated products (iii, Figure 4) of core-fucosylated (2,4)tri-antennary glycans (from structures 13b/11b in Table 2) and of core-fucosylated bi-antennary glycans with a bisecting GlcNAc (from structures 12b/11a in Table 2) co-eluted on NP HPLC at 6.09 NPGU (iii, Figure 2d). The degalactosylated product (vi) (Figure 2d) appeared to originate from core-fucosylated tetra-antennary glycans with a bisecting GlcNAc although no such galactosylated parent glycans were readily observed in earlier digests. However, it seemed probable that this family of complex glycans existed in the original brain sample as a number of minor peaks below the detection limit for detailed analysis.

(ii) Glycosidase digestions of the kidney Na^+,K^+-ATPase preparation. Although the oligomannosidic family $(Man)_{5\text{-}9}$ was detected in the kidney preparation, this class of glycan did not dominate the NP HPLC profile (Figure 3a; peaks 1–5) with only Man_6 (peak 2) present in a significant quantity. The oligomannosidic glycans were completely digested to Man_1 (2.41 NPGU, peak off scale with void material, Figure 3b) by jack bean α-mannosidase, confirming these assignments.

The subsequent digestion of the complex-type oligosac-

Table 3. Assignment of glycan structures from total Na^+,K^+-ATPase-enriched preparation of kidney.

Isobaric composition	*NP HPLC glucose units*[a]	*Structure*[b]	*Ref.#*[c]
H5 N2	6.15 (6.16)		1
H6 N2	7.04 (7.05)	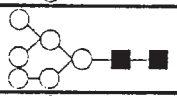	2
H7 N2	7.94 (7.91)		3
H8 N2	8.82 (8.81)	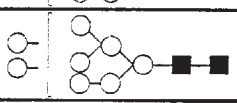	4
H9 N2	9.52 (9.49)		5
H5 N4	7.05 (7.00)	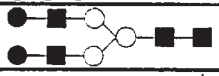	6
H5 N4 F	7.48 (7.43)	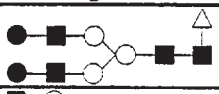	7
H3 N5	5.64 (5.66)	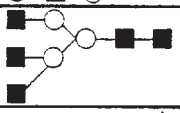	8
H3 N5 F	6.07 (6.06)	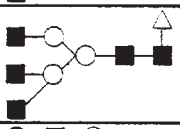	9
H6 N5	8.26 (8.22)	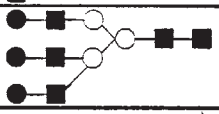	10
H6 N5 F	8.65 (8.61)	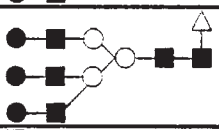	11
H3 N6*	6.39 (6.34)	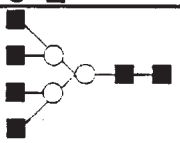	12
H3 N6 F*	6.79 (6.71)	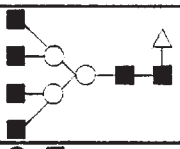	13
H7 N6	9.65 (9.63)	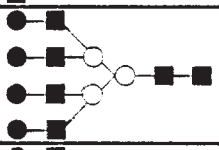	14
H7 N6 F	9.98 (9.93)	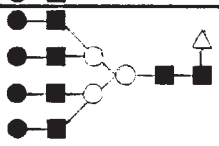	15

Table 3. *(continued)*

Isobaric composition	*NP HPLC glucose units*[a]	*Structure*[b]	*Ref.#*[c]
H8 N7	10.77	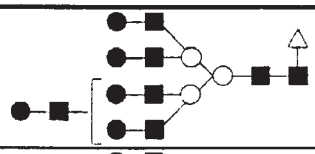	16
H8 N7 F	11.06	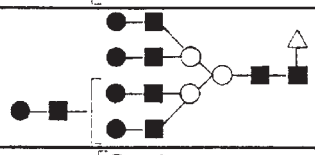	17
H9 N8	12.12	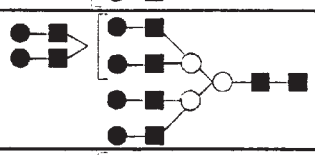	18
H9 N8 F	12.40	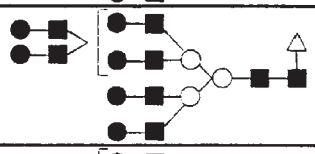	19
H10 N9	13.10	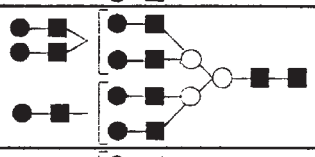	20
H10 N9 F*	13.35	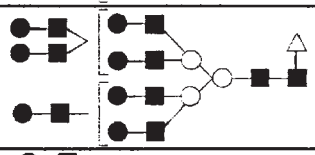	21
H11 N10*	14.04	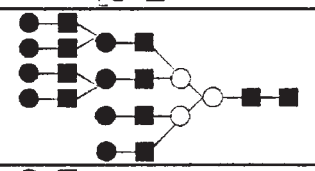	22
H11 N10 F*	14.31	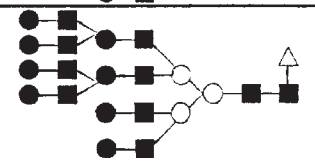	23

[a]The NP HPLC glucose units of standards were listed in parenthesis where these data were available.
[b]The squares represent N-acetyl glucosamine, white circles mannose, black circles galactose and triangles fucose.
[c]The reference number cross-references this table with the oligosaccharide peaks of Figure 3.
* = Not detected by mass spectrometry.
The illustrated glycans (structures 16–23) represent the most likely arm-specific distribution of the linear or branched polylactosamines.

charides from the kidney preparation is explained below. NP HPLC profiles and subsequent glycosidase digestions indicated that these glycans were dominated by fully galactosylated tetra-antennary structures, with and without core fucose (Figure 3b, peaks 15 and 14 respectively), that could be extended by up to four *N*-acetyl-lactosamine [(Galβ1-4GlcNAcβ1-3)$_{1-4}$] units (Figure 3b, peaks 16–23).

The putative fully galactosylated tetra-antennary glycan containing three *N*-acetyl-lactosamine units, with and without core fucose (Figure 3b, peaks 21 and 20, respectively),

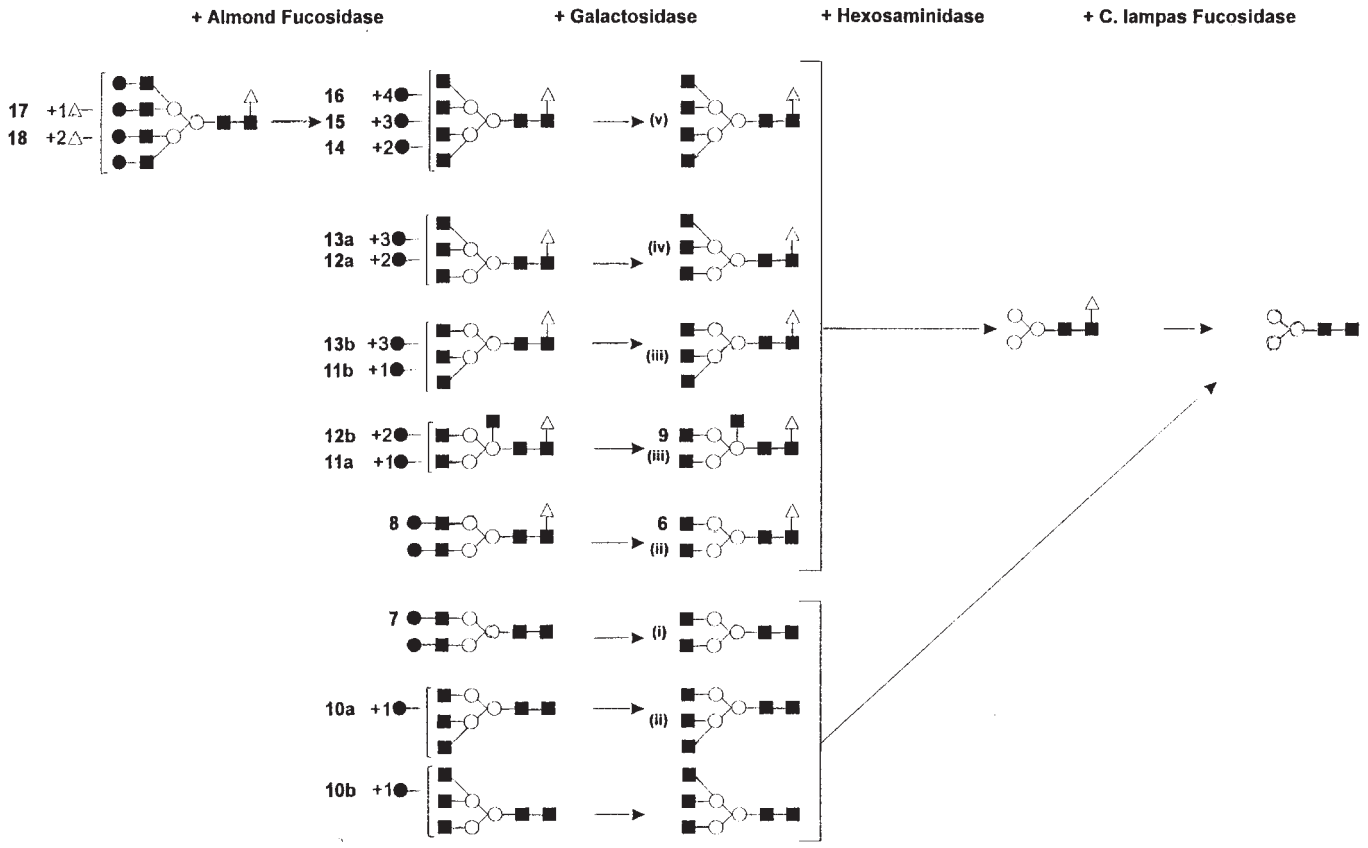

Figure 4. Schematic representation of the sequential digestion of the most abundant complex-type N-linked glycans from the brain Na^+,K^+-ATPase preparation to their pentasaccharide core structure. Numbers in bold refer to structures present in the original neutralised Na^+,K^+-ATPase sample, listed in Table 2. (i)–(v) refer to the peaks in Figure 2d. The squares represent N-acetyl glucosamine, white circles mannose, black circles galactose and triangles fucose.

completely shifted on digestion with endo β-galactosidase (to product peaks iv and iii, respectively, Figure 3c). However, the putative tetra-antennary glycans, with and without core fucose, containing two and four additional *N*-acetyl-lactosamine units were entirely resistant to this enzyme (i.e., peaks 19 & 18 and 23 & 22, respectively, did not shift: Figure 3c). There are a number of possibilities for this observed endo β-galactosidase resistance [21], such as (i) outer-arm fucosylation, (ii) sulphation and (iii) the presence of branched 'polylactosamine' extensions. (i) can be discounted by the results (see Figure 3f below) which indicated that, when present, the only fucose in the kidney glycans was on the core. This was supported by the compositional data (Table 1) showing that not more than one deoxyhexose (fucose) was present in any glycan detected in the kidney preparation. (ii) can be discounted by the fact that all the acidic glycans were neutralised by *A.ureafaciens* neuraminidase (see above). The data are, therefore, consistent with the presence of a mixture of branched and linear tetra-antennary 'polylactosamine' structures. These are resistant and susceptible to endo β-galactosidase respectively [21]. 'Polylactosamine' is used here to indicate the presence of one or more *N*-acetyl-lactosamine units additional to those constituting the elementary outer-arm sequence.

The sequential digestion of the putative polylactosamine series (each structure without or with a core fucose) is described below and summarised in Figure 5. It is proposed that the glycans with two and four additional *N*-acetyl-lactosamine units carried them as *branched* extensions (Table 3, structures 18 & 19 and 22 & 23, respectively) which were resistant to endo β-galactosidase. In contrast, the glycans with one and three additional *N*-acetyl-lactosamine units each contained *one linear N*-acetyl-lactosamine extension which was susceptible to this enzyme (Table 3, structures 16 & 17 and 20 & 21, respectively). Thus, on digestion with endo β-galactosidase, the mono- and tri-*N*-acetyl-lactosamine containing glycans (Figure 3b, peaks 16 & 17 and 20 & 21, respectively) collapsed with the loss of the one linear *N*-acetyl-lactosamine unit and its internal galactose (forming peaks i & ii and iii & iv, respectively, Figure 3c). The remaining, unsubstituted galactoses of the smaller structural pair were hydrolysed by bovine testes β-galactosidase to form the degalactosylated tetra-antennary glycan, with and without core fucose (thus collapsing into the

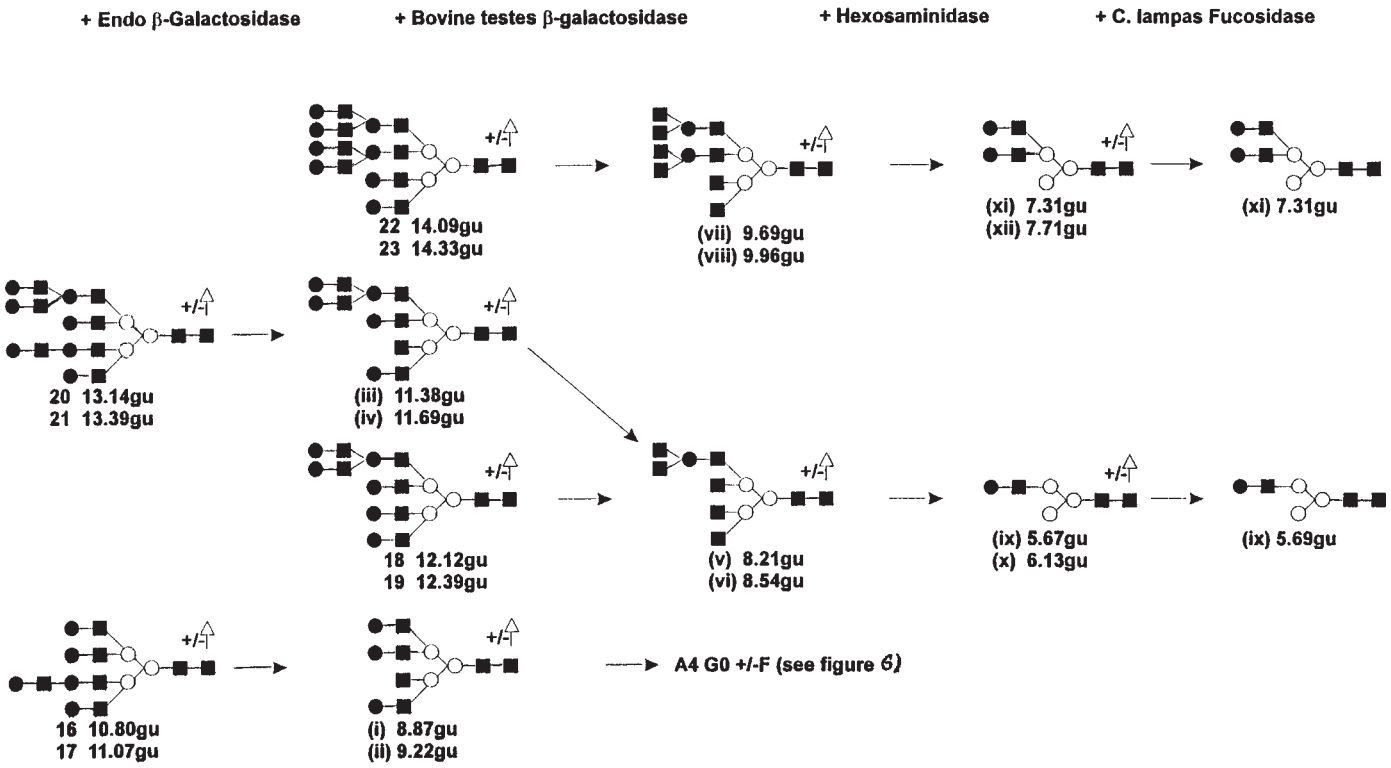

Figure 5. Schematic representation of the sequential digestion of assigned kidney Na^+,K^+-ATPase polylactosamine-containing N-linked glycans. The numbers refer to structures present in the original neutralised Na^+,K^+-ATPase sample, listed in Table 3. Roman numerals refer to the digestion products of Figure 3. Symbols are as described in the legend to Figure 4. Normal phase HPLC glucose units ('gu') are also shown for each glycan.

pre-existing peaks, 13 & 12, respectively, at 6.79 and 6.39 NPGU: Figure 3d).

The larger products of the endo β-galactosidase digest (iii and iv, Figure 5) lost their non-reducing terminal galactose residues following digestion with bovine testes β-galactosidase (forming structures v and vi, Figures 3d and 5). The glycans originally carrying two (endo β-galactosidase-resistant) *N*-acetyl-lactosamine units (18 & 19, in Figures 3c and 5) were also digested by this galactosidase to the same products. Similarly, the glycans originally carrying four (endo β-galactosidase-resistant) *N*-acetyl-lactosamine units (22 and 23, in Figures 3c and 5) were digested by this enzyme, also losing, in turn, their non-reducing terminal galactose residues (forming structures vii and viii, Figures 3d and 5). On subsequent digestion with jack bean β-*N*-acetyl-hexosaminidase, structures that were either mono- or di-substituted with *N*-acetyl-lactosamine units on the trimannose-chitobiose core were formed (ix and x, xi and xii, respectively, Figures 3e and 5). Digestion of these glycans with *C. lampas* α-fucosidase caused exclusively the formation of the non-core fucosylated products (ix and xi, Figure 3f and 5).

The trimannose-chitobiose digestion product that was di-substituted with *N*-acetyl-lactosamines (structure xi, 7.31 NPGU) eluted significantly later than the standard biantennary glycan possessing one *N*-acetyl-lactosamine residue on each antenna (7.00 NPGU). This suggested that both of those remaining *N*-acetyl-lactosamine residues were on one antenna. In addition, the NPGU value for this compound is consistent with the substitution of the 6- but not the 3-arm by comparison with the NP HPLC of 2,6- (6-arm) and 2,4- (3-arm) substituted triantennary glycans. From these data it can be predicted that the original, branched tetra-lactosamine extensions (Table 3, structures 22 and 23) were both likely to be located on the 6-arm. By analogy, if the less highly substituted structures (18-21, Table 3) were precursors of these, the *N*-acetyl-lactosamine extensions would be located on the 6-, rather than the 3-, arm.

The digestion of the remaining complex-type glycans from the kidney Na^+,K^+-ATPase-enriched preparation is summarised in Figure 6. The β-galactosidase digestion showed that no significant partially galactosylated tetra-, tri- or biantennary glycans could be resolved from the mixture by HPLC (though MALDI-MS was able to detect a few minor peaks, e.g., of compositions $H_4N_5+/-F$ and H_5N_6, which were consistent with such structures, see Table 1 and Figure 10a, below). The triantennary glycans in the kidney were found to have '2,4' branching only, based on NPGU values (which would have been higher for '2,6'

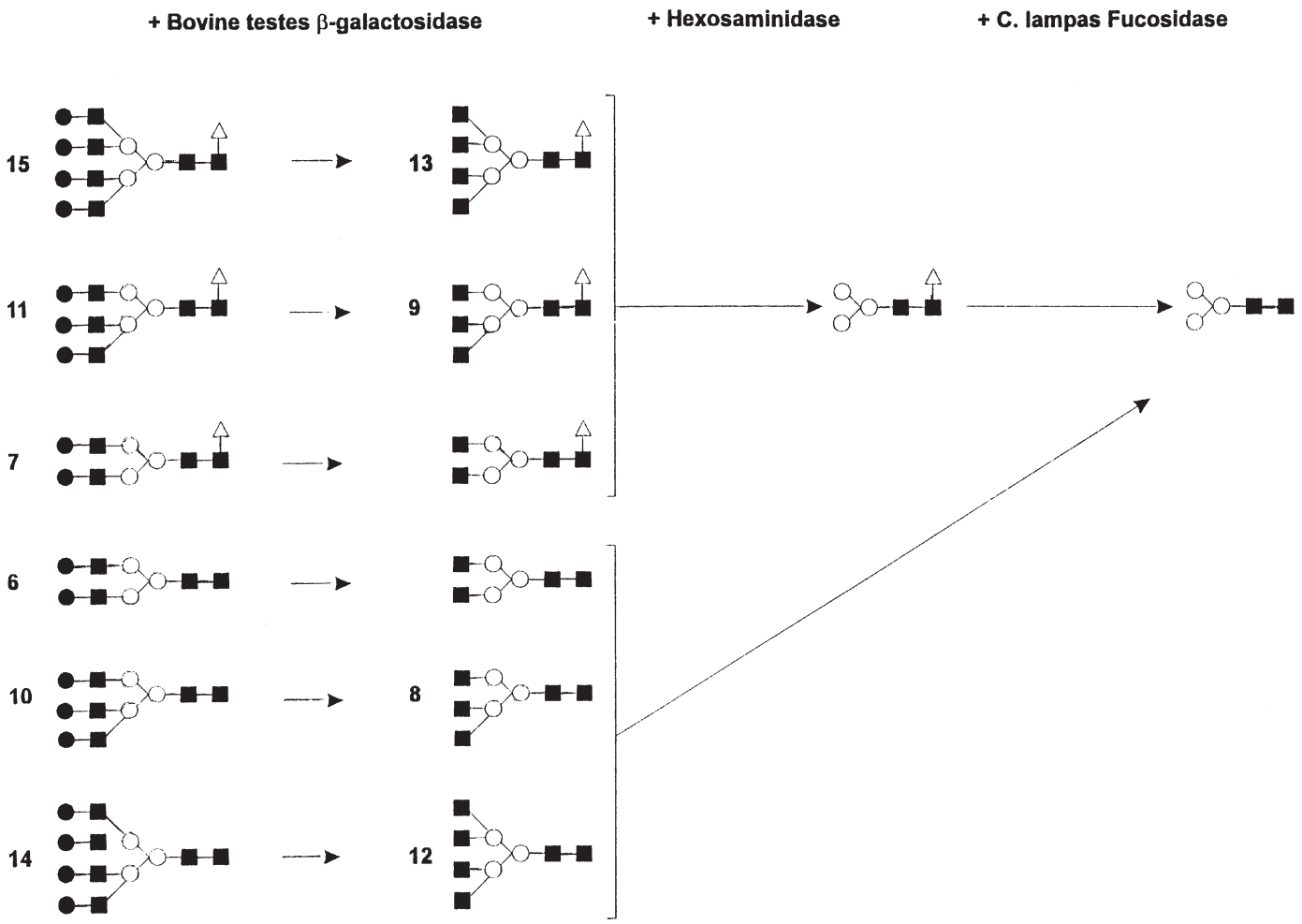

Figure 6. The sequential digestion of assigned kidney Na^+,K^+-ATPase complex-type N-linked glycans not containing polylactosamines. Numbers in bold refer to structures present in the original neutralised Na^+,K^+-ATPase sample, listed in Table 3. Symbols are as described in the legend to Figure 4.

structures) and sensitivities to arm-specific exoglycosidase digestions [20]. Unlike the preparation from brain tissue, no outer-arm fucosylation, generating Lewis x-type structures, was found in the kidney Na^+,K^+-ATPase.

Characterisation of Na^+,K^+-ATPase-enriched preparations

The study was extended so that carbohydrates associated with particular subfractions of the Na^+,K^+-ATPase-enriched samples could be identified. Essentially this involved the separation and identification of protein subunits by SDS-PAGE, followed by release of *N*-glycans, where present, from appropriate bands 'in-gel', using PNGase F. The released glycans were subsequently isolated and purified for analysis, in this case by MALDI-MS.

A 15 × 15 cm gel, loaded with 30 μg protein from both the brain and kidney preparations, was subjected to SDS-PAGE (see Methods) and was stained with Coomassie blue (Figure 7). The kidney sample separated into a high molecular weight doublet (M_r 98 and 92 kDa) and a more diffuse band at M_r 61–51 kDa. The brain sample also had a high molecular weight doublet (M_r 101 and 96 kDa) although, unlike the kidney, the bands were not of equal intensity. A major band was apparent at 51 kDa as well as a diffuse region (52–47 kDa) in the brain sample. The higher molecular weight species reacted with the α subunit antibodies and the smaller species with the β subunit antibodies (Figure 8). In detail, the kidney preparation reacted mainly with α-1 and β-1, with traces of β-2 also being identified, whereas the brain sample bound α-2, α-3, β-1 and β-2 with traces of α-1 also being detected.

N-terminal sequencing was performed in addition to Western blotting to confirm further the presence and identity of the α subunits. The two closely migrating bands in the α region of both the brain and kidney preparations were excised separately and termed 'α-upper' and 'α-lower' for the higher and lower apparent M_rs respectively. The N-ter-

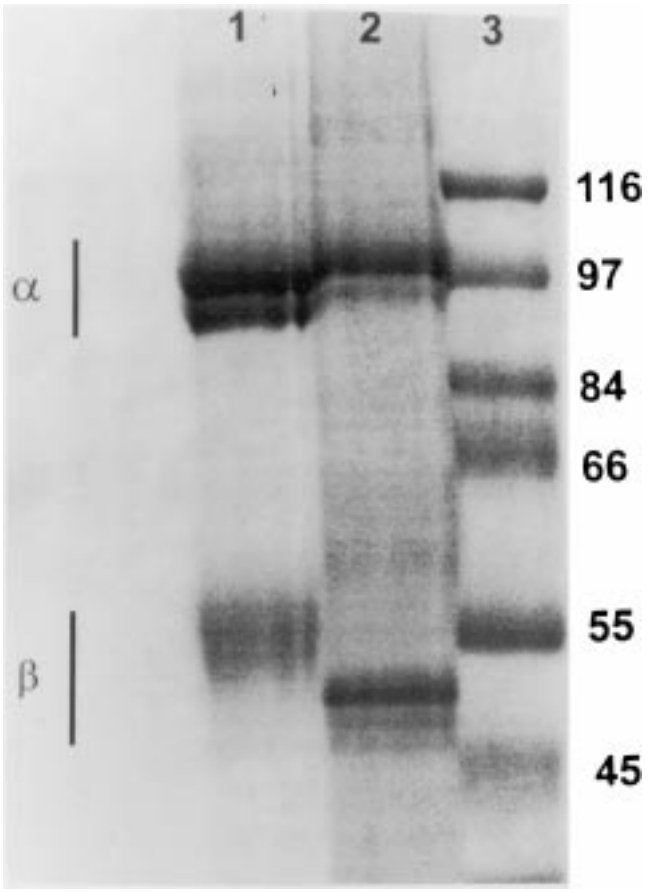

Figure 7. Coomassie blue stained SDS-PAGE of brain and kidney Na^+,K^+-ATPase preparations. 30 μg protein from each of the kidney (lane 1) and brain (lane 2) preparations were loaded. The 92–101 kDa and 47–61 kDa regions coincide with the α and β subunit regions of Na^+,K^+-ATPase respectively (see Figure 8). The molecular weights (kDa) of marker proteins (lane 3) are indicated on the right.

minal sequences were determined for each band, except brain α-lower, for which no clear data were obtained (this was probably due to insufficient starting material as this band was relatively weakly stained by Coomassie blue in comparison to other species of similar molecular weight). Both bands analysed from kidney tissue resulted in the assignment of a single sequence, 14 amino acid derivatives in length (GRDKYEPAAVSEHG), corresponding to those predicted from the cDNA of rat α-1 [22]. No other amino acid derivatives were detected in the kidney α-subunit band. The brain α-upper band yielded a major sequence of 8 amino acid derivatives (GREYSPAA), identified as the N-terminus of rat α-2 subunit, together with a fragmented minor sequence (K_DK) corresponding to the appropriate α-3 subunit sequence predicted from cDNA nucleotides [22].

In addition, MALDI-MS peptide mass mapping [14] of the doublet and peptide sequencing by tandem MS [15]—see 'Methods'—clearly identified the rat α-1 Na^+,K^+-ATPase subunit with a sequence coverage of 41% and no contamination was detected (data not shown). Using the same techniques, the kidney β-subunits were also found to be essentially free from detectable levels of contaminating proteins. The specific activity of an identical Na^+,K^+- ATPase preparation from kidney was 1060μmol/mg/h (as recorded by the rate of NADH oxidation in a linked enzyme assay) [8].

Similarly MALDI-MS peptide mass mapping identified all three of the rat α-subunits of Na^+,K^+-ATPase in the brain sample running at 101 kDa and 96 kDa with sequence coverages of 29% for α-1, 25% for α-2 and 29% for α-3 and again no contaminating proteins were detectable (data not shown). This was further confirmed by peptide sequencing using tandem MS. These MS techniques revealed that the region of the gel that contained the brain β-subunits did contain calcium/calmodulin-dependent protein (CAM) kinase type II α-chain, present in a minor capacity.

Mass spectra were obtained for the neutral/desialylated oligosaccharides released by PNGase F (and neutralised by *A.ureafaciens* neuraminidase) from the higher (α-subunit-containing) and lower (β-subunit-containing) molecular weight regions of the gel from both the brain (Figure 9) and kidney (Figure 10) preparations. The isobaric monosaccharide compositions obtained in each case are summarised in Table 1. These showed generally good agreement with the structures predicted from the HPLC and glycosidase analyses of the total preparation as depicted in Tables 2 and 3.

In the case of the brain preparation, compositions consistent with the main proposed structures were indeed seen as major components by MALDI-MS in both the high and low molecular weight bands. In addition, minor components were detectable, usually in both bands, many of which possessed two or three deoxyhexoses (fucoses), indicative of one or two fucoses located on the outer-arms (in addition to the one on the core), and, by analogy, sensitive to almond meal α-fucosidase (Figure 2c). Thus an array of the glycans in the brain preparation can be expected to carry the Lewis x structure, typical of those seen in whole rat brain tissue [23]. A few additional, but minor, non-core-fucosylated glycans were also detected.

In addition, with the kidney sample, compositions (Table 1, Figure 10) consistent with many of the major proposed structures from the whole preparation (Table 3) were seen. The polylactosamine-containing glycans of the lower molecular weight band distinguished it from the higher molecular weight band, although they were observed in relatively less abundance than in the HPLC study of the total preparation. A few minor glycans, essentially of the complex-type and detected by MS in the higher molecular weight band, were not resolved in the HPLC analyses. No hexuronic acid or sulphate residues were found in either tissue preparation in any analysis.

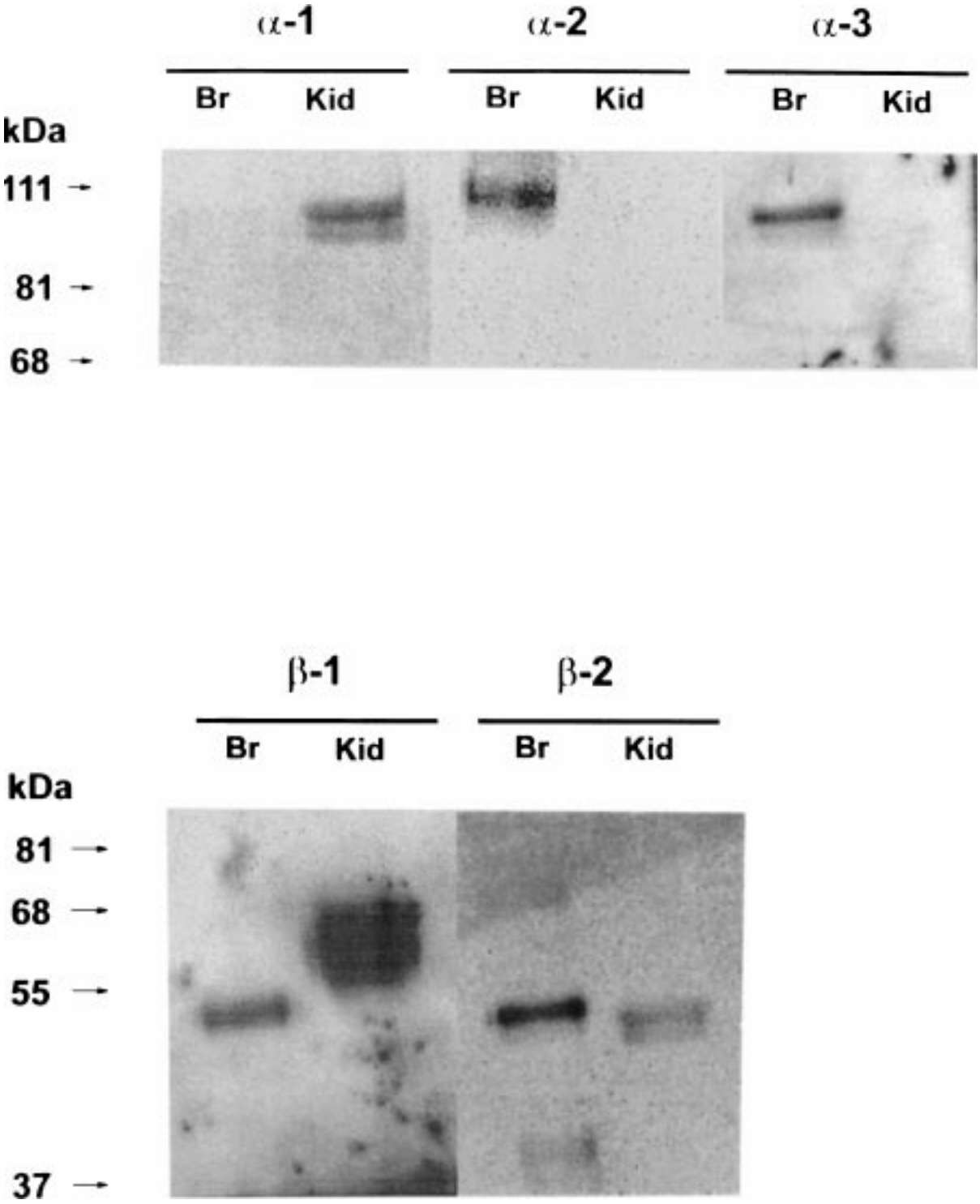

Figure 8. Detection of brain and kidney Na^+,K^+-ATPase subunits by Western blot analysis. 6 μg protein from each of the brain (Br) and kidney (Kid) preparations were separated by SDS PAGE, electroblotted onto PVDF and reacted with antibodies specific to either α-1, α-2, α-3, β-1 or β-2 Na^+,K^+-ATPase subunits. The molecular weights (kDa) of marker proteins are indicated on the left.

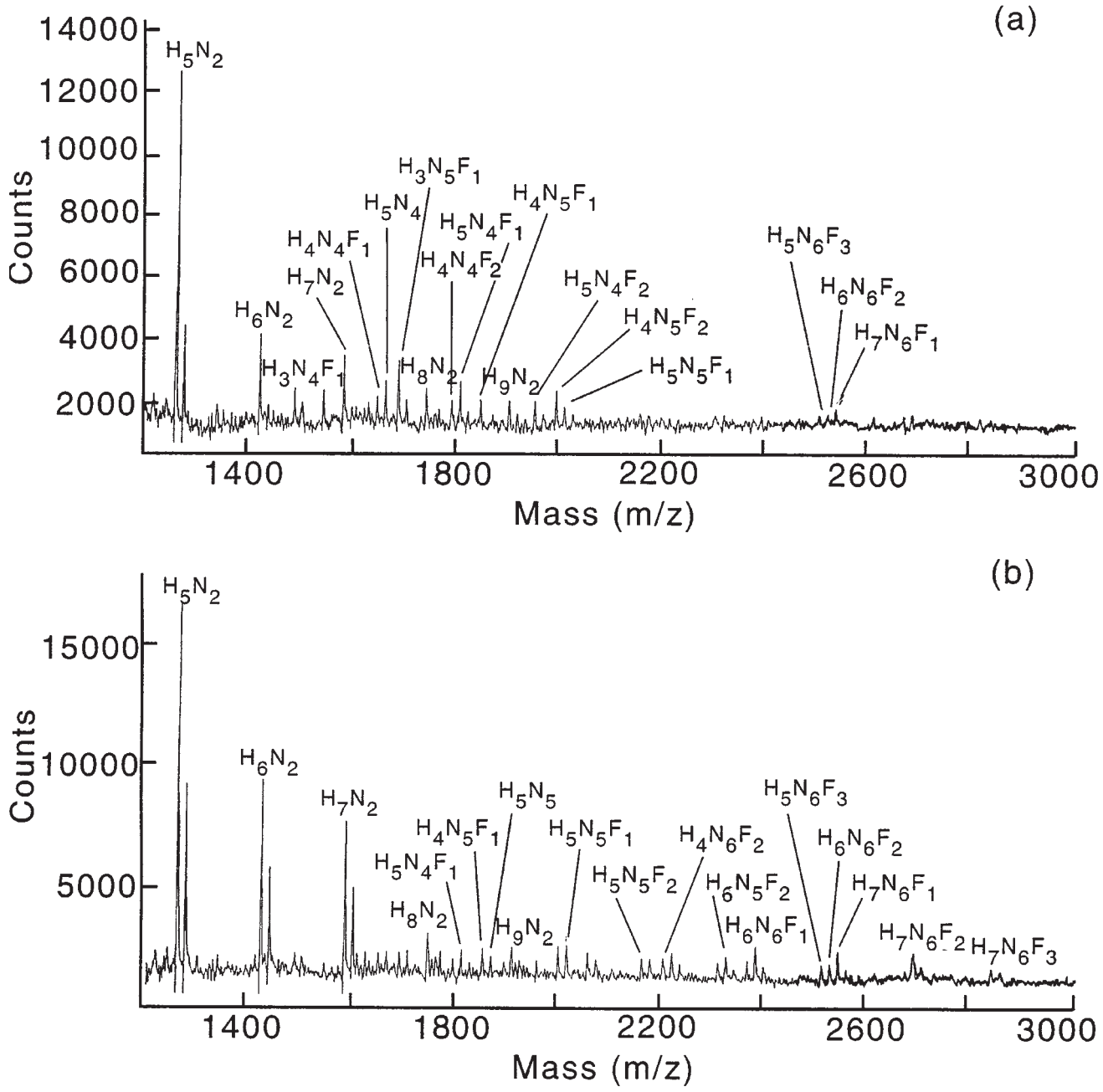

Figure 9. Mass spectra of glycans, released by PNGase F and treated with sialidase, from the brain Na^+,K^+-ATPase - enriched preparation after SDS-PAGE: (a) high molecular weight region (101 kDa) and (b) low molecular weight region (51 kDa). For clarity, not all peaks have been labelled with their isobaric monosaccharide compositions.

Discussion

The Na^+,K^+-ATPase-enriched preparations from brain and renal tissue exhibited tissue-specific glycosylation, both qualitatively and quantitatively. Oligosaccharides from the brain preparation were more neutral than those from the kidney (54 and 33% neutral glycans respectively) although the existing anionic species in both tissues were all neutralised by sialidase. Thus the glycans in neither tissue were associated with anionic groups such as sulphates, which can be common, particularly in the brain [24]. The preponderance of the kidney-associated acidic glycans being sialylated was in agreement with earlier studies on the β-subunit [9,25,26].

The natural neutral and sialidase-neutralised glycans from the brain and kidney Na^+,K^+-ATPase-enriched preparations, however, were very different. The brain sam-

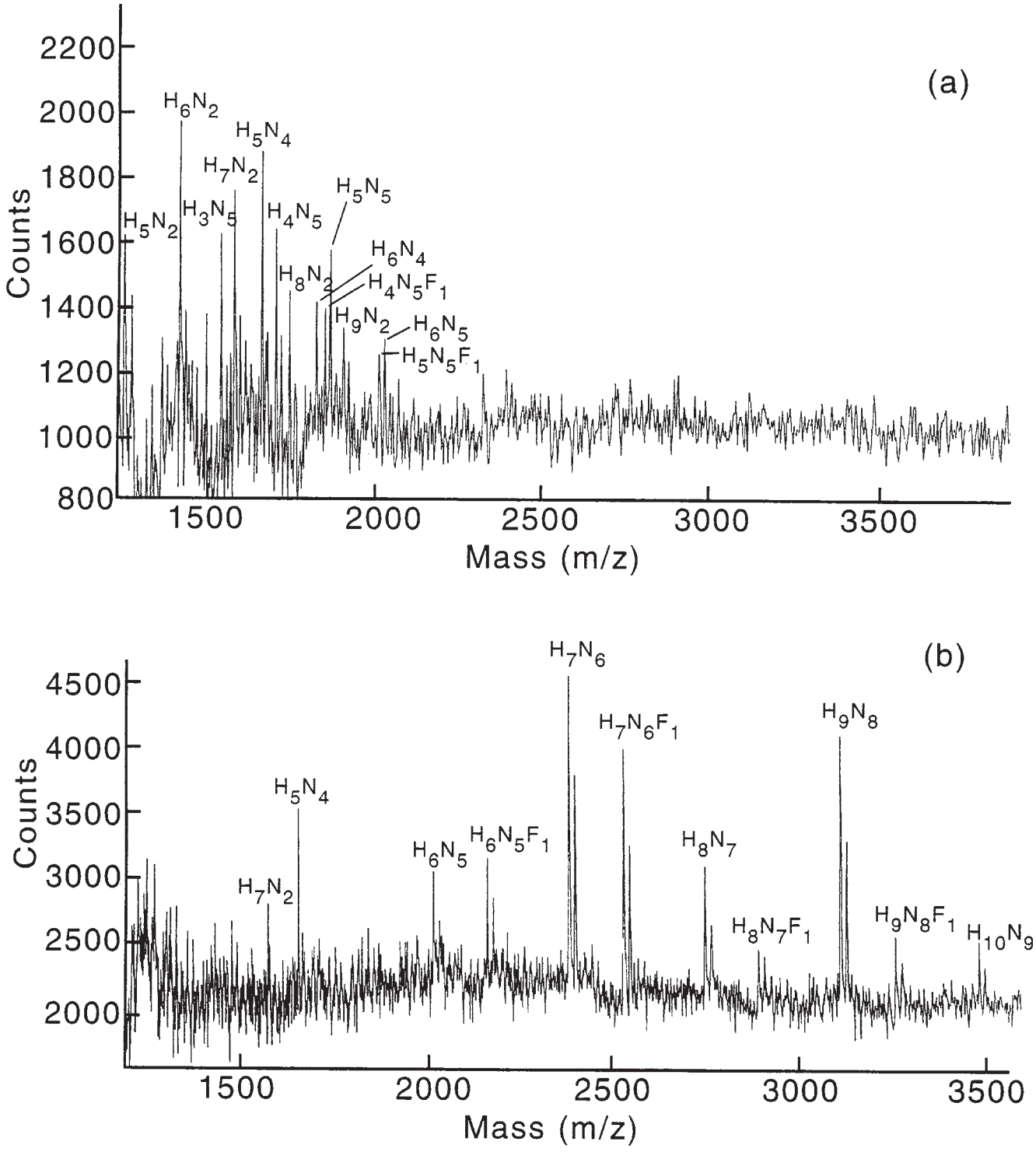

Figure 10. Mass spectra of glycans, released by PNGase F and treated with sialidase, from the kidney Na^+,K^+-ATPase - enriched preparation after SDS-PAGE: (a) high molecular weight region (92–98kDa) and (b) low molecular weight region (51–61 kDa).

ple was predominantly oligomannosidic whereas that from renal tissue was dominated by mannosidase-resistant, complex-type glycans. Those complex-type glycans that were present in the brain preparation were all core fucosylated (with the exception of the galactosylated biantennary structure) whereas all the complex-type oligosaccharides of kidney existed as two series, one core fucosylated and the other non-fucosylated. The tri-antennary family of complex glycans existed as both (2,4)- and (2,6)-branched structures in the brain preparation whereas in the kidney it was present only as the (2,4)-branched form. This suggested competition between *N*-acetylglucosaminyltransferases IV and V (GnT-IV and -V) in brain but with only GnT-IV active in kidney. There was no evidence for outer-arm fucosylation in the kidney whereas several of the tetra-antennary glycans of the brain sample possessed one or two outer-arm fucose residues, generating the Lewis x structures.

The renal preparation was associated with a series of high molecular weight oligosaccharides, which were not present in brain, some of which were shown in the present study to be sensitive to endo β-galactosidase, indicating the presence of linear lactosaminylglycan units. Treuheit et al. [9], in their analysis of the complex-type glycans of the β subunit of kidney Na^+,K^+-ATPase, also found significant quantities of tetra-antennary glycans with polylactosamine extensions. In the absence of sequencing information, it was not possible for them to assign the distribution of the lactosamine units, but it was assumed that they all formed linear arm extensions. The use of additional techniques, such as sequential glycosidase digestions, in the present study, enabled many of the lactosamine units also to be assigned as branched, rather than linear, extensions. Thus the results presented here are in broad agreement with, as well as significantly extending, their data. No attempt was made to study site specificity of glycosylation in view of the lack of such specificity shown for the β-subunit from kidney [9]. It is interesting to note that, in the present study, some members of the polylactosamine series showed considerable relative abundance by HPLC but were relatively less abundant by mass spectrometry. This may have been due to difficulties in extracting such large sugars from polyacrylamide gels during sample preparation prior to MALDI-TOF or reflect a greater abundance in the total preparation.

The results of this study substantiated, with definitive glycan structures, the lectin blot data of Benallal and Anner [8,27], implicating, in particular, that the Na^+,K^+-ATPase-containing fractions from the brain preparation were highly oligomannosidic in comparison with those from the kidney. It was suggested by Treuheit et al. [9] that because of the ubiquitous nature of Na^+,K^+-ATPase, the N-linked oligosaccharides described in their study would, not only further define the covalent structure of the β1-subunit from lamb and dog kidney, but also serve as a model for the glycans involved in extracellular communications in many other tissues. Clearly the present results detailing tissue *specificity* of glycosylation for the Na^+,K^+-ATPase-enriched preparations point to, and substantiate the view that such a characteristic, on this scale, may alternatively be useful for targeting tissues as in the therapeutics.

The comprehensive glycan analyses of the present study have been focussed on rat brain and kidney tissues because of the fundamental importance of Na^+,K^+-ATPase for the excitable activity of nervous tissue and in regulating fluid reabsorption and electrolyte movement in the kidney. However, the considerable analytical differences in glycosylation observed for these two tissue preparations, despite the sequence homologies of Na^+,K^+-ATPase isoforms, suggest a broad potential for tissue specificities of Na^+,K^+-ATPase glycosylation upon which lectins could operate with selectivity. The efficiency would be enhanced by the abundant nature of this enzyme. Further, earlier lectin-blotting studies [8] gave similar comparative results when brain and kidney Na^+,K^+-ATPase preparations from other species, including human and rabbit, were studied. Thus this tissue-specificity of glycosylation showed species independence with the host-cell glycosylation machinery dictating the glycoform repertoire.

The glycosylation of the Na^+,K^+-ATPase β subunit has been shown to be functionally important in the folding and expression of Na^+,K^+-ATPase [28,29]. The β-2 subunit has been shown to be the adhesion molecule on glia (AMOG) [6], and so the oligosaccharides of this molecule in brain tissue may be important in mediating recognition events. It is known that the monoclonal antibodies, L3 and L4, recognising oligomannosidic carbohydrate epitopes on certain neural adhesion molecules, including AMOG, interfere with cell interactions [30]. This is consistent with the quantitative significance of oligomannosidic glycans in the brain preparation in the present study, and as was indicated by the earlier lectin work [8]. Na^+,K^+-ATPase is highly enriched at CNS synapses and the present results show that, through the oligomannose-type glycans, it possesses the same general glycosylation pattern observed in other synaptic glycoproteins, notably belonging to the glutamate receptor family [31]. In this situation it appears that the tissue-specificity of glycosylation particularly reflects the available repertoire of glycosyltransferases, rather than their individual accessibility to different glycosylation sites.

It is generally accepted that the α-subunits of Na^+,K^+-ATPase are not glycosylated, though some studies have favoured the presence of carbohydrate, including those from Pedemonte's group [32,33], necessitating the proposal for cytosolically oriented N-linked sugars. The issue has been controversial on account of the assessed purities of the various preparations. The MS results of the present study suggest that N-linked glycans were observed in association with the higher molecular weight bands, coincidental in their gel-running with the α-subunits of the

Na^+,K^+-ATPases studied. The results thus substantiate the findings of Benallal and Anner [8] that such bands from similar Na^+,K^+-ATPase-enriched preparations were reactive with GNA and DSA lectins, for the brain and kidney preparations, respectively. Using a variety of techniques, no impurities were established in these higher molecular weight bands in the present study. However, the possibility of several co-migrating glycoproteins, each in sub-detectable abundance (or conceivably with an N-terminal blocked), contributing to the carbohydrates that were detected, cannot be ruled out in the absence of defined glycosylation sites on the α-subunit.

Acknowledgements

This work was supported by a BBSRC grant and a CASE award from Oxford GlycoSciences (1), to R.A.C.C. a DAA predoctoral and an EMBO long-term postdoctoral fellowship (to B.K.) and SNSF grant No. 31-37552.93 (to B.M.A. & M.B.). The authors are grateful to Dr. K. Drickamer for the N-terminal sequencing, to Dr A. Hunter for the acquisition and processing of the MS carbohydrate data and to Mr. B. Matthews for performing the hydrazinolysis. We thank Profs. Matthias Mann and Ed Southern for access to the mass spectrometers used for peptide sequencing and glycan analyses, respectively.

References

1 Lingrel JB, Kuntzweiler T (1994) *J Biol Chem* **269:** 19659–62.
2 Geering K (1991) *FEBS Lett* **285:** 189–93.
3 Fambrough DM, Lemas MV, Hamrick M, Emerick M, Renaud KJ, Inman EM, Hwang B, Takeyasu K (1994) *Am J Physiol* **266:** C579–89.
4 Jorgensen PL, Andersen JP (1988) *J Membrane Biol* **103:** 95–120.
5 Fiedler B, Scheiner-Bobis G (1996) *J Biol Chem* **271:** 29312–20.
6 Gloor S, Antonicek H, Sweadner KJ, Pagliusi S, Frank R, Moos M, Schachner M (1990) *J Cell Biol* **110:** 165–74.
7 Shyjan AW, Levenson R (1989) *Biochemistry* **28:** 4531–35.
8 Benallal M, Anner BM (1995) *Bioscience Reports* **15:** 21–36.
9 Treuheit MJ, Costello CE, Kirley TL (1993) *J Biol Chem* **268:** 13914–19
10 Küster B, Wheeler SF, Hunter AP, Dwek RA, Harvey DJ (1997) *Anal Biochem* **250:** 82–101.
11 Dzhandzhugazyan KN, Jorgensen PL (1985) *Biochim Biophys Acta* **817:** 165–73.
12 Laemmli UK (1970) *Nature* **227:** 680–85.
13 Matsudaira P (1987) *J Biol Chem* **262:** 10035–38.
14 Mann M, Hojrup P, Roepstorff P (1993) *Biol Mass Spectrom* **22:** 338–45.
15 Wilm M, Shevchenko A, Houthaeve T, Breit S, Schweigerer L, Fotsis T, Mann M (1996) *Nature* **379:** 466–69.
16 Ashford D, Dwek RA, Welply JK, Amatayakul S, Homans SW, Lis H, Taylor GN, Rademacher TW (1987) *Eur J Biochem* **166:** 311–20.
17 Patel T, Bruce J, Merry A, Bigge C, Wormald M, Jaques A, Parekh RB (1993) *Biochemistry* **32:** 679–93.
18 Bigge JC, Patel TP, Bruce JA, Goulding PN, Charles SM, Parekh RB (1995) *Anal Biochem* **230:** 229–38.
19 Guile GR, Wong SYC, Dwek RA (1994) *Anal Biochem* **222:** 231–35.
20 Guile GR, Rudd PM, Wing DR, Prime SB, Dwek RA (1996) *Anal Biochem* **240:** 210–26.
21 Scudder P, Hanfland P, Uemura K-I, Feizi T (1984) *J Biol Chem* **259:** 6586–92.
22 Shull G.E, Greeb J, Lingrel JB (1986) *Biochemistry* **25:** 8125–32.
23 Chen Y-J, Wing DR, Guile GR, Dwek RA, Harvey DJ, Zamze S (1998) *Eur J Biochem* **251:** 691–703.
24 Wing DR, Rademacher TW, Field MC, Dwek RA, Schmitz B, Thor G, Schachner M (1992) *Glycoconjugate J* **9:** 293–301.
25 Miller RP, Farley RA (1988) *Biochim Biophys Acta* **954:** 50–57.
26 Munakata H, Schmid K, Collins JH, Zot AS, Lane LK, Schwartz A (1982) *Biochem Biophys Res Commun* **107:** 229–31.
27 Benallal M, Anner BM (1994) *Experientia* **50:** 664–68.
28 Beggah AT, Jaunin P, Geering K (1997) *J Biol Chem* **272:** 10318–26.
29 Zamofing D, Rossier BC, Geering K (1988) *J Membrane Biol* **104:** 69–79.
30 Fahrig T, Schmitz B, Weber D, Kucherer-Ehret A, Faissner A, Schachner M (1990) *Eur J Neurosci* **2:** 153–61.
31 Clark RAC, Gurd JW, Bissoon N, Tricaud N, Molnar E, Zamze SE, Dwek RA, McIlhinney RAJ, Wing DR (1998) *J Neurochem* **70:** 2594–605.
32 Pedemonte CH, Sachs G, Kaplan JH (1990) *Proc Natl Acad Sci. USA* **87:** 9789–93.
33 Pedemonte CH, Kaplan JH (1992) *Biochemistry* **31:** 10465–70.

Received 17 June 1999, revised 13 August 1999, accepted 16 August 1999